

Article

Preparation of Graphene Conductive Fabrics and the Study of Their Degradation Behavior

Wei Xiong ¹, Yingze Jiang ¹, Guinian Huang ¹, Yinyan Hou ¹, Yuxin Yang ¹, Yanping Niu ¹, Junxin Yin ¹ and Hongwei Liu ^{2,*} 

¹ Hubei Key Laboratory of Biomass Fiber and Eco-Dyeing & Finishing, College of Chemistry and Chemical Engineering, Wuhan Textile University, Wuhan 430073, China

² School of Chemical Engineering and Technology, Sun Yat-sen University, Zhuhai 519082, China

* Correspondence: liuhw35@mail.sysu.edu.cn

Abstract: Graphene has excellent electromagnetic, mechanical, thermal, and optical properties and has been widely applied in materials science, biomedicine, physics, energy storage, chemistry, and textile fields all over the world. In this paper, graphene conductive fabrics were prepared by the impregnation method, and ascorbic acid was used as a reducing agent. Ammonia-cotton blended fabric was used as the base material. Results indicated that graphene had been successfully covered on fabrics according to XRD and SEM analysis. The optimum technological parameters for preparing graphene conductive fabrics were: impregnation five times, reduction temperature at 95 °C, the ascorbic acid concentration of 0.06 mol/L, and the reduction time was 40 min. A corrosion study indicated that rGO fabrics could be partly corroded in 3 wt.% NaCl solution, leading to a decrease in resistivity. However, the conductive ability of rGO fabric changed little with time due to the good stability of rGO.

Keywords: graphene; fabric; graphene coated fabric; degradation



Citation: Xiong, W.; Jiang, Y.; Huang, G.; Hou, Y.; Yang, Y.; Niu, Y.; Yin, J.; Liu, H. Preparation of Graphene Conductive Fabrics and the Study of Their Degradation Behavior. *Coatings* **2022**, *12*, 1432. <https://doi.org/10.3390/coatings12101432>

Academic Editor: Stefano Caporali

Received: 16 August 2022

Accepted: 23 September 2022

Published: 29 September 2022

Publisher's Note: MDPI stays neutral with regard to jurisdictional claims in published maps and institutional affiliations.



Copyright: © 2022 by the authors. Licensee MDPI, Basel, Switzerland. This article is an open access article distributed under the terms and conditions of the Creative Commons Attribution (CC BY) license (<https://creativecommons.org/licenses/by/4.0/>).

1. Introduction

Textiles have been widely used in daily life due to their many advantages, such as flammable static electricity [1,2]. With the fast development of technologies and higher human needs, multifunctional textiles show excellent performance for special requirements [3–5]. Conductive fabrics are very important as one part of multifunctional textiles, and they play key roles in textiles achieving their special function [3,6]. The combination of graphene and fabrics promotes the fast development of conductive fabrics and increases their extensive application [7–11].

Graphene comes from graphite and is usually prepared by chemical methods, and currently, graphene can be large-scale prepared easily due to the improvement in preparation method [12]. It is well known that graphene has many good characteristics, such as excellent electromagnetic, mechanical, thermal, and optical [13–17]. So, graphene has been applied in many areas. Graphene, graphene oxide (GO) and restore oxidation graphene (rGO) are commonly used to prepare different materials with special aims. Mostly, GO, and rGO are good choices due to their good dispersibility in water. And GO can be part reduced to prepare rGO [18]. Therefore, graphene, GO, and rGO can be the ideal materials for the preparation of conductive fabrics [19–21].

The main methods of used to prepare graphene conductive fabrics include impregnation [22,23], vapour phase deposition [24], electrochemical deposition [25], vacuum filtration [26] and electrophoresis [27]. Compared to the other methods, the impregnation method has many advantages, such as easy operation, low energy consumption, and low pollution. During the preparation process of the graphene conductive fabrics by impregnation, GO is first combined with the fibers and then reduced to rGO. The commonly used

reduction GO methods can be divided into physical and chemical reductions [28,29]. Thermal reduction [30], ultraviolet reduction [31], and microwave reduction [32] are types of physical reduction. However, there are still some disadvantages to physical reduction, i.e., they are complex to operate, require a high reduction environment (e.g., thermal reduction in an inert gas environment), and can easily cause damage to the fibers during the reduction process [33]. Chemical reduction is operated simply and easily controlled [34–36].

In this paper, graphene conductive fabrics were prepared by the impregnation method. Ammonia-cotton blended fabric with strong mechanical properties is used as the base material [37]. Graphene conductive fabrics have the advantages of low production cost, good dispersity, and affinity with fabric. Fabrics attached to GO are reduced by a highly reducing REDOX method using ascorbic acid, an environmentally friendly reducing agent. This preparation method is environmentally friendly, with a low cost of raw materials, no pollution in the preparation process, high-quality products, and high yield [38,39]. The treated fabrics have potential excellent electrical conductivity, anti-electromagnetic shielding, anti-bacterial, and flame retardant properties [30,40].

2. Experimental

2.1. Reagents and Materials

Ammonia-cotton blended fabric, ascorbic acid, and NaCl were supplied by Shanghai Sinopharm Group. GO dispersion with a concentration of 0.5 mg/mL was obtained from Nanjing Xian Feng Nanomaterials Technology Co., LTD (Nanjing, China).

2.2. Preparation of Graphene Conductive Fabrics

The fabric with a size of 1.5 cm × 4 cm was soaked in GO suspension at room temperature for 30 min and then dried at 60 °C for 25 min [41]. This process was repeated five times to increase the adsorption capacity of GO. The reduction of the GO-coated fabrics was carried out at 95 °C in the ascorbic acid. The prepared fabrics were washed with distilled water several times and then dried in a vacuum at 60 °C.

2.3. Degradation of Graphene Conductive Fabrics

The degradation behavior study of the prepared graphene conductive fabrics was tested in 3.5 wt.% NaCl solution. Normal oxidation of graphene conductive fabrics in the air was the control. The prepared graphene conductive fabrics were immersed in a 3.5% NaCl solution, and the resistivity was measured after 1, 2, and 3 h of testing. The surface morphologies of graphene conductive fabrics after degradation were observed by SEM. The resistivity of the prepared graphene conductive fabrics was measured after 24, 48, and 72 h of exposure to air.

2.4. Characterizations

SEM images were conducted using an 800-07334 Feiner desktop scanning electron microscope produced by PHENOMWORLD (Eindhoven, The Netherlands). XRD produced by Japanese Science Corporation (Rigaku, Tokyo, Japan) was employed to analyze the substance and structure of the prepared materials. The 4-probe tester is equipment for measuring semiconductor resistivity and square resistance using the 4-probe principle. The advantages of the equipment are simple operation, accurate and fast measurement data, wide measurement range, and good stability. The resistivity calculation formula is shown below:

$$\rho = R \frac{S}{L} \quad (1)$$

where ρ was the resistivity, R was the resistance, S was the cross-section area of fabric, and L was the length of fabric.

2.5. Electrochemical Measurements

A saturated calomel electrode (SCE) (Smartlab SE R0232, Shanghai Huayu Instrument, Shanghai, China) used as the reference electrode and the platinum electrode as the counter electrode were employed in a three-electrode system. Cyclic voltammetry (CV) and charge-discharge tests were carried out to study the electrochemical performance of the prepared materials.

3. Results and Discussion

3.1. SEM Observation

SEM images corresponding to the microstructure of fabrics are shown in Figures 1 and 2. Figure 1a–g shows the samples that were dipped 1–7 times at $1500\times g$, respectively, and Figure 2a–g shows the samples that were dipped 1–7 times at $500\times g$. Figures 1a and 2a are used as the control in the morphologies analysis due to the different dipping times. As shown in Figure 1, a thin monolayer with irregular edges is observed, and rGO is successfully adhered to the surface of the fabric after dipping. As the dipping times increase from 1–4, a discontinuous and sparse layer containing rGO on the surface of fabrics increases successively. However, the graphene lamellar completely covers the surface of the fibers, and the continuous block and irregular edge on the smooth surface of fibers appear after the fifth impregnation. When the impregnation times continue to increase, the surface of the fabric gradually appears the stacking of reduced graphene oxide, which may have a certain impact on the conductive effect of the fabric. It can be preliminarily judged that five times impregnation can meet the basic requirements of preparing graphene conductive fabrics.

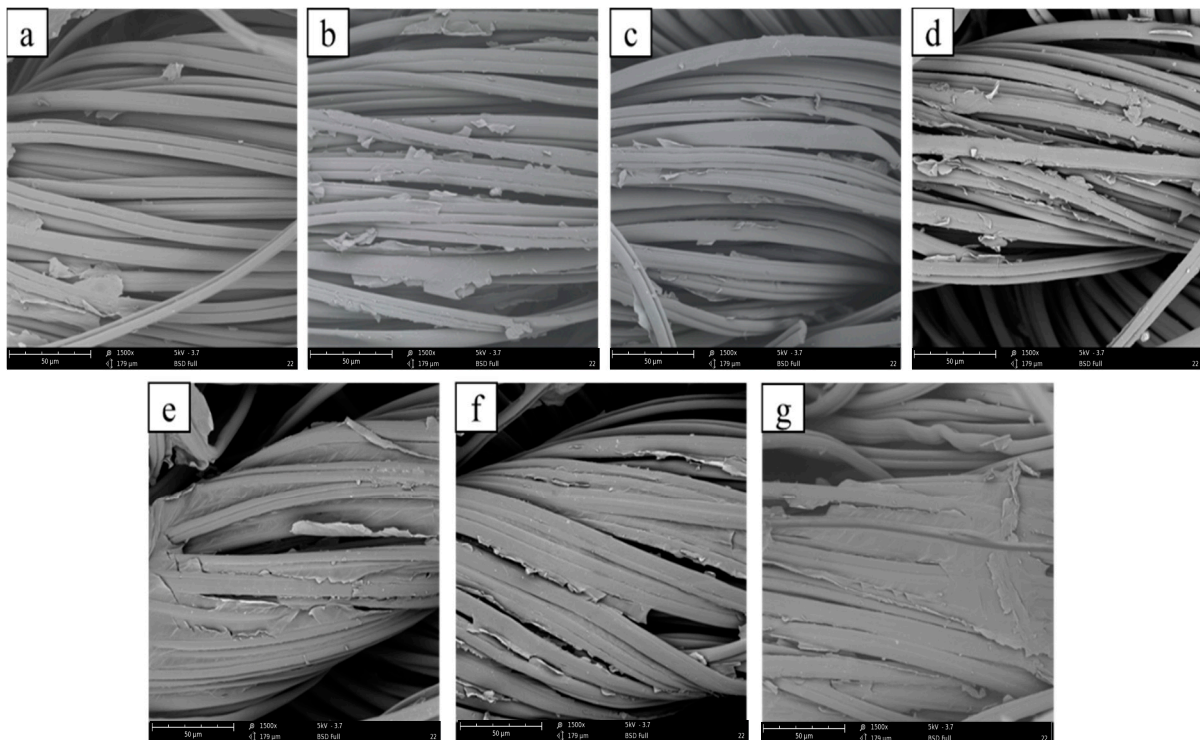


Figure 1. SEM images of conductive graphene fabric soaked 1–7 times ($1500\times$, (a–g) were soaked 1–7 times respectively).

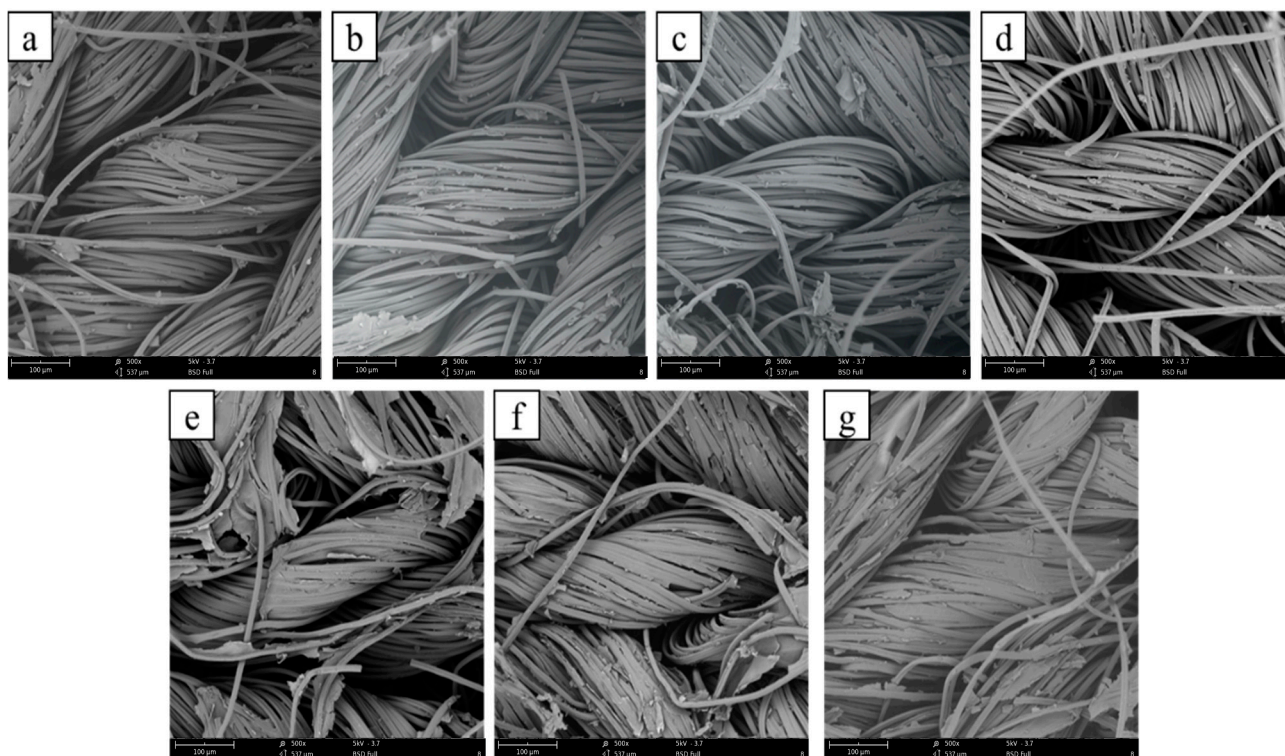


Figure 2. SEM images of conductive graphene fabric soaked 1–7 times (500 \times , (a–g) were soaked 1–7 times respectively).

3.2. XRD Analysis

XRD analysis results of the prepared materials are presented in Figure 3. A low and sharp diffraction peak at about 11° indicates that GO is attached to the fabric. Meanwhile, there is a high-intensity diffraction peak at about 22° , demonstrating that most of the GO-coated on the fabrics has been reduced to rGO. As impregnation times increase, the graphene diffraction peaks shift to the left. The diffraction peak around 42° can be due to the stacking of GO, then leading to the formation of a small amount of graphite after reduction [18,42,43]. The above XRD characteristic peaks fully illustrate the successful preparation of conductive fabrics, i.e., the graphene oxides have been successfully coated on the fabrics and then are partly reduced.

There are two active hydroxyl groups on the double bond of the ascorbic acid quinary ring, and it is easy to dissociate two protons. Most oxygen-containing functional groups of GO exist in the form of epoxy or hydroxyl groups. In terms of the epoxy group, under the attack of ascorbic acid, one end forms hydroxyl, and the other end is connected with ascorbic acid oxygen anion. Then the other hydroxyl on the double bond of the ascorbic acid five-membered ring is removed from the water molecule by the hydroxyl formed after the back attack of the ring opening to form an intermediate [44]. Finally, the intermediate may recover the C=C conjugate system by removing small molecules in the reaction to obtain rGO, while ascorbic acid is oxidized to dehydroascorbic acid [45]. The reduction of the hydroxyl group is similar to the epoxy group. The Hydroxyl group is replaced by an oxygen anion of ascorbic acid, accompanied by a secondary attack on the back, and then reduced by an elimination reaction. Dehydroascorbic acid is easily further decomposed into gulonic acid and other oxidation products. From the XRD results, it can be seen that there are small amounts of oxygen-containing groups in the fabric after ascorbic acid reduction, and hydrogen bonds can be formed between gulonic acid and oxygen-containing groups, which destroys the π - π stacking between graphene layers and makes it more stable.

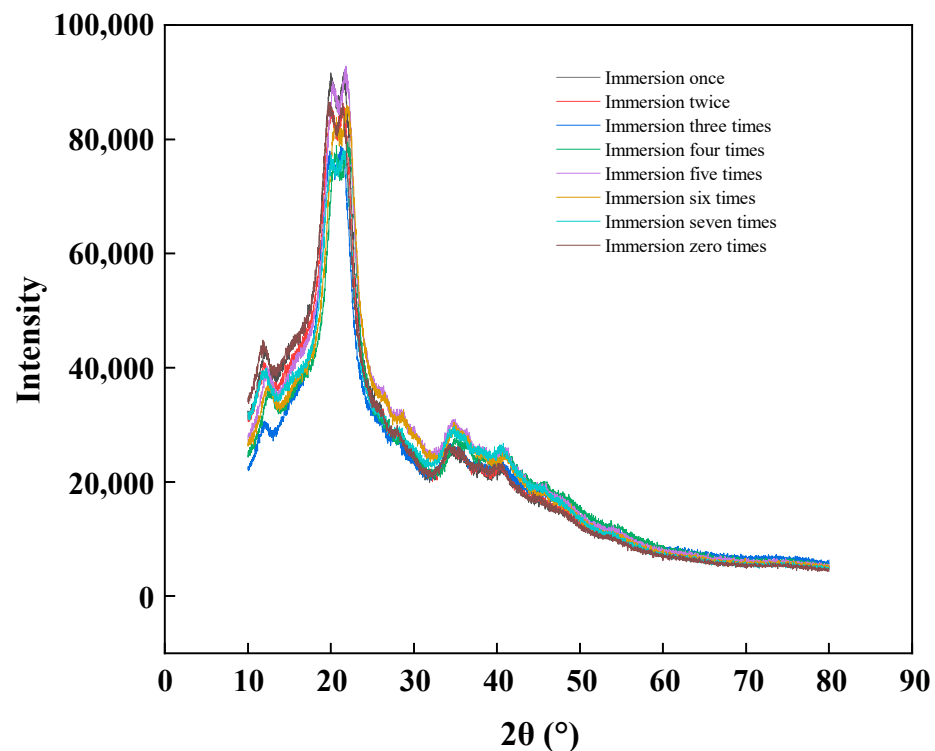


Figure 3. X-ray diffraction images of fabric coated by graphene with different impregnation times.

3.3. Effects of Impregnation Times on Fabric Conduction

Four probe tester is used to measure the resistivity of the fabric with different impregnation times, and the corresponding results are shown in Figure 4. For the first impregnation, the resistivity of treated fabric is high and over the range of the four-probe tester because of the attachment of little amount of GO on fabrics. The adsorbed graphene is not enough to form a good conductive layer with a large area. So, the fabrics are almost not conductive, and the fabric resistivity is large. As the increase of impregnation times from 2 to 5, the resistivity of the fabrics decreases and becomes stable. After the fifth repetition, the resistivity of the fabrics is around $6.8 \Omega \cdot \text{m}$ and then changes little. The impregnation and drying process is repeated, but the resistivity of the fabrics does not decrease significantly. With the increase of impregnation times, the amount of graphene oxide adsorbed on the fabric gradually increases. After reduction, the obtained rGO conductive layer is good, so the resistivity of the conductive fabric shows a downward trend. When the impregnation times reached five, it can be seen from Figure 1 that some graphene precipitates appear on the surface of the fabric, indicating that the adsorbed graphene on the fabric has reached saturation. Therefore, the resistivity of the fabrics does not decrease significantly with the increase in impregnation times. The precipitation and stacking of graphene can affect the electrical conductivity of the fabrics. In conclusion, the best number of impregnation times for preparing graphene conductive fabrics is five.

3.4. Effects of Reduction Times

Before the reduction of prepared materials, the samples that impregnation five times are carried out. After different reduction times in ascorbic acid, the resistivities of the prepared fabrics are measured using the four-probe tester to investigate the relationship between the reduction time and the resistivity of the fabrics, and the results are shown in Figure 5. It is seen that the resistivity of the fabrics decreases gradually as the increase of reduction time. After 40 min, the resistivity of the fabric is around $5.6 \Omega \cdot \text{m}$. So, the reduction time over 40 min has little effect on the resistivity of the fabrics. The resistivity at reduction times of 50 and 60 min is slightly higher than that at 40 min. When the reduction time is short, graphene oxide adsorbed on the fabrics cannot be completely reduced, so the

conductive layer is incomplete, leading to a large fabric resistivity. With the increase in reduction time, the adsorbed film of graphene oxides is good when the reduction time is over 40 min. Therefore, the resistivity of the conductive fabrics is lowest after 40 min. When the reduction time continues to increase, the formed rGO conductive layer can be partially damaged at a high temperature, resulting in a slight increase in fabric resistivity. In conclusion, the best time for reducing GO is 40 min.

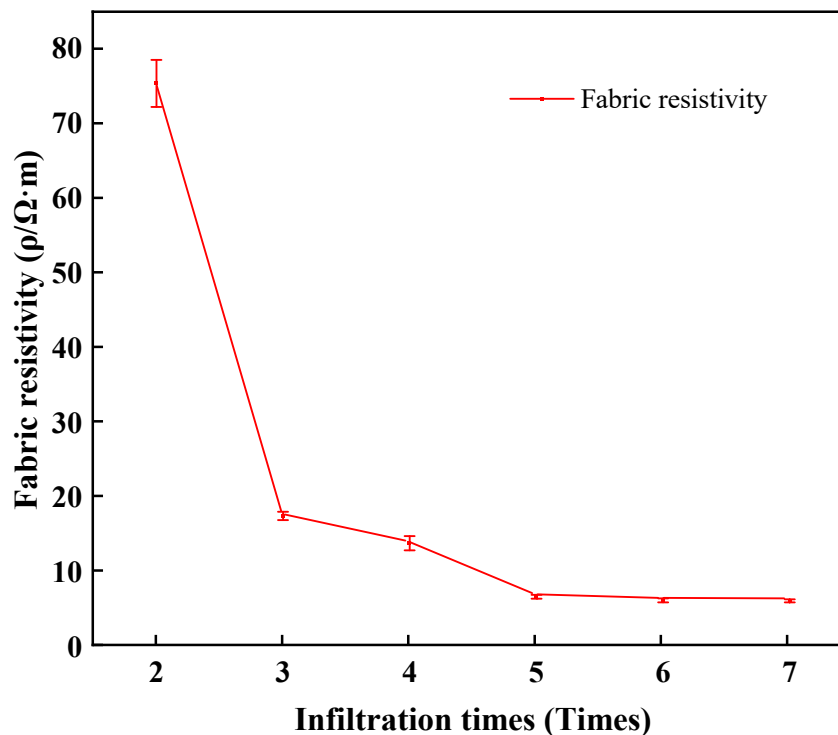


Figure 4. Fabric resistivity with different impregnation times.

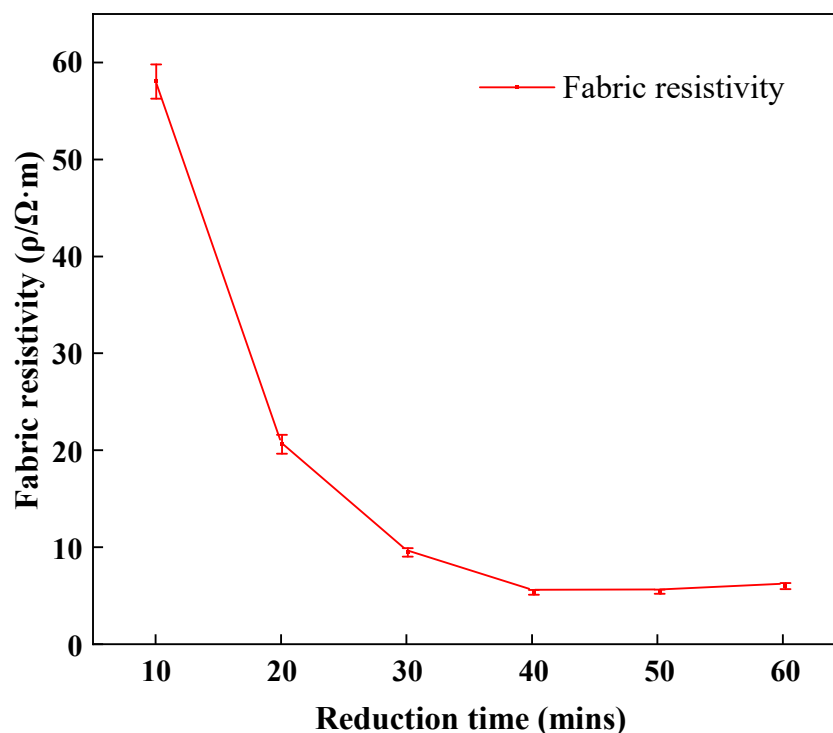


Figure 5. Fabric resistivity of different samples with different reduction times.

3.5. Effects of Reducing Agent Concentrations on Fabric Resistivity

Effects of the different reducing agent concentrations on fabric resistivity are studied. The number of impregnation times of GO is five, corresponding to a reduction time of 40 min, and the test temperature is 95 °C. The corresponding results are shown in Figure 6. The fabric resistivity decreases as the increase of reducing agent concentration. However, the reducing agent with a concentration of more than 0.06 mol/L has little effect on the resistivity of the fabrics. When the concentration of ascorbic acid is low, the concentration of the reducing agent is insufficient to completely reduce the GO adsorbed on the fabric surface. From the change of resistivity, it can be seen that the ascorbic acid, with a concentration of 0.06 mol/L, is sufficient to completely reduce GO on the fabrics. Therefore, with the increase of the ascorbic acid concentration, the resistivity of the fabrics is almost unchanged. So, the optimal concentration of ascorbic acid as a reducing agent for preparing graphene conductive fabrics is 0.06 mol/L.

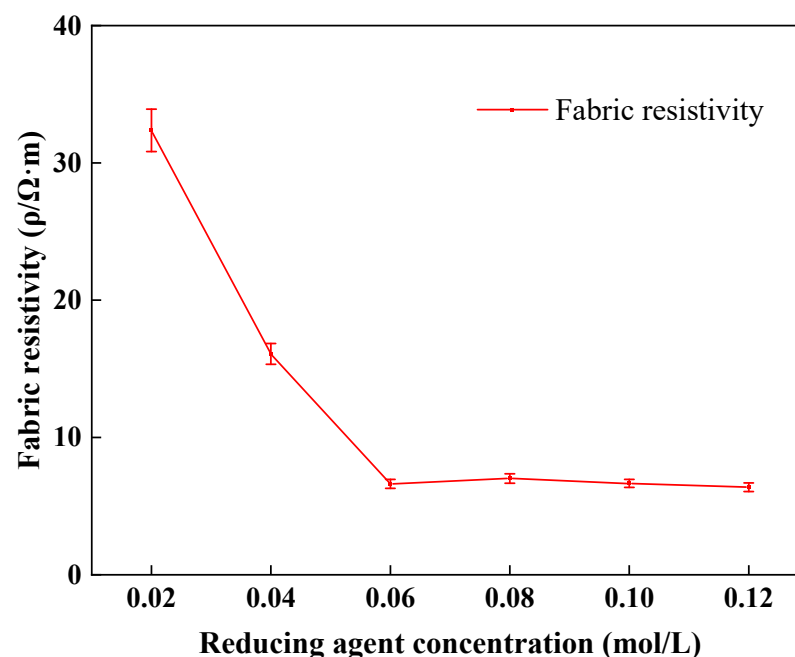


Figure 6. Fabric resistivity of the prepared samples with different reducing agent concentrations.

3.6. Effects of Reduction Temperature on Fabric Resistivity

After impregnation five times, the fabric is immersed in 0.06 mol/L ascorbic acid for 40 min, and the reduction temperature is changed from 45 to 95 °C. The images of different samples are shown in Figure 7. The resistivity of samples at 45, 55, 65, 70, 75, and 80 °C cannot be measured. This is because a low temperature causes a slow reaction rate, so a continuous conductive film on the fabrics has not yet formed, leading to a large resistivity. As seen in Figure 7, the color of the prepared fabric gradually changes with the increase of temperature from gray-brown to black-grey, and the reduction degree of samples increases gradually from 45~90 °C.

The relationship between the resistivity and reduction time is shown in Figure 8. When the reduction temperature is 90 °C, the GO on fabrics can be completely reduced in 60 min. As the increase of reduction time, the resistivity of the fabric changes little with a value of 11 $\Omega\cdot m$. This is because the extension of reaction time makes more oxygen-containing functional groups combine with the oxidation product of ascorbic acid, gulonic acid, rather than be reduced. Meanwhile, when the reduction temperature is 85 °C, the reduction of GO has not been complete in 90 min, and the fabric resistivity is slightly higher than that at 90 °C. As shown in Figures 6 and 8, although the fabric can be completely reduced at 90 °C by prolonging the reduction time, the resistivity at 90 °C is less than that at 95 °C. Therefore, the optimal reduction temperature is 95 °C.

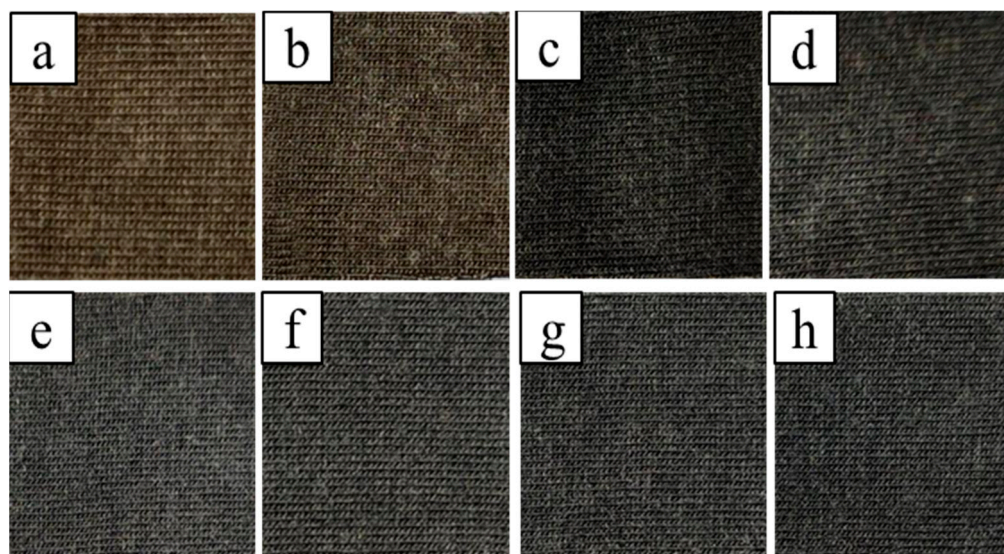


Figure 7. SEM images of samples at different reduction temperatures: 500 \times (a) 45 $^{\circ}$ C, (b) 55 $^{\circ}$ C, (c) 65 $^{\circ}$ C, (d) 70 $^{\circ}$ C, (e) 75 $^{\circ}$ C, (f) 80 $^{\circ}$ C, (g) 85 $^{\circ}$ C, (h) 90 $^{\circ}$ C.

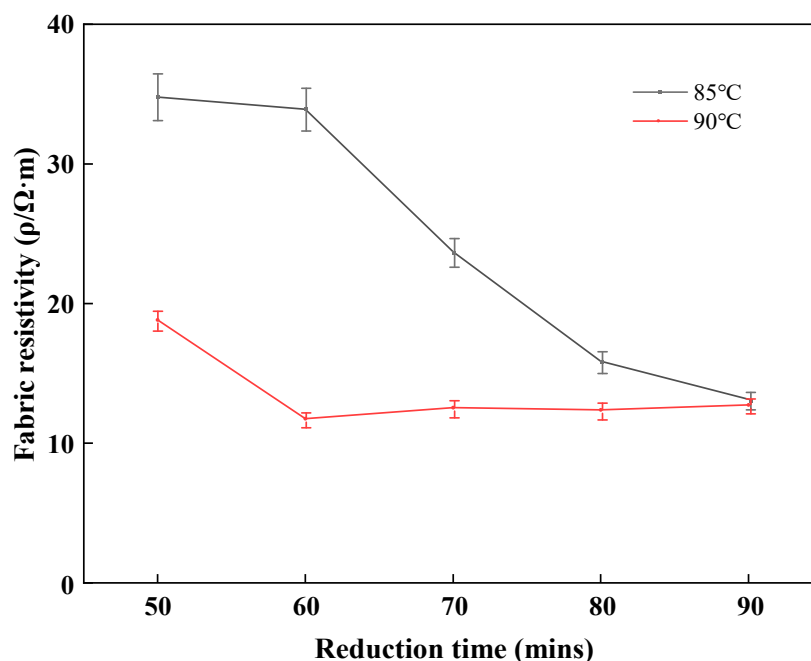


Figure 8. Fabric resistivity of prepared samples at different reduction times and temperatures.

3.7. Cyclic Voltammetry Tests

The scanning speeds of CV tests are 50 and 100 mV/s, respectively [46]. The CV curves of the prepared samples are shown in Figure 9. CV curve shows a regular symmetrical shape, which indicates that the prepared material has good cyclic properties during the charging-discharging processes. The reaction on the GO conductive fabric is reversible, and the conductive fabric has the potential to be a capacitor [47]. It can be seen from the specific capacitance calculation formula that the specific capacitance is proportional to the area surrounded by the CV curve. The CV curve of this sample is a waist circle with a small area. Therefore, the prepared sample capacitance is not sufficient as a supercapacitor, and it still needs further improvement.

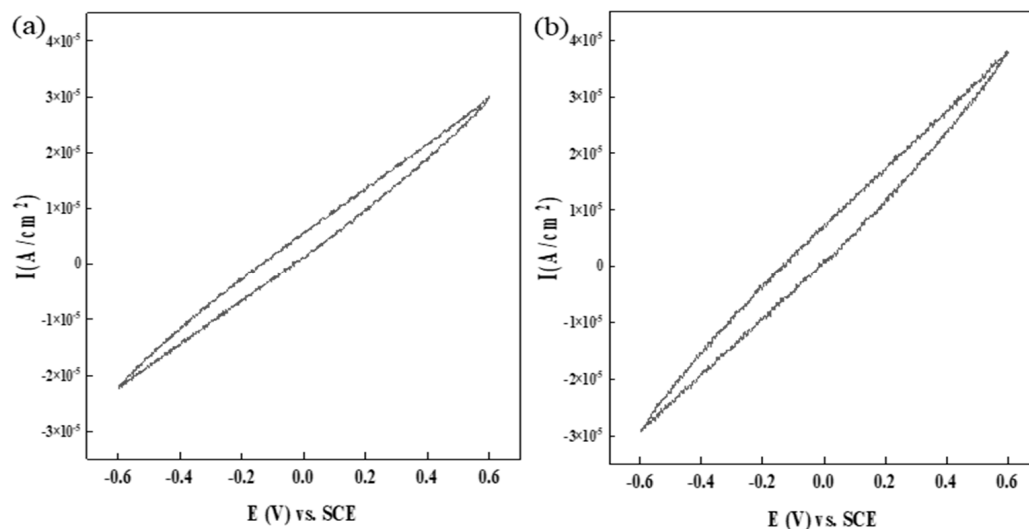


Figure 9. Cyclic voltammetry curves of prepared samples with different scanning rates: (a) 50 mV/s, (b) 100 mV/s.

3.8. Charge and Discharge Test

Graphene conductive fabric is also investigated by a constant current charge-discharge test, and the result is shown in Figure 10. The prepared rGO fabrics are charged and discharged at a current of 10 μA . The discharge starts at the voltage of 0.8 V vs. SCE, while the charge starts at 0 V vs. SCE. The charging-discharging process can be repeated. During this process, the electrochemical performance almost does not decay, and the redox reaction on the graphene fabric is completely reversible. The charge-discharge voltage changes with time in a symmetrical triangular distribution, but its charge-discharge curve is not perfectly linear, only quasi-linear. These are mainly because graphene contains some oxygen-containing functional groups, which can provide a certain amount of pseudocapacitor, further confirming the results of CV curves [48,49].

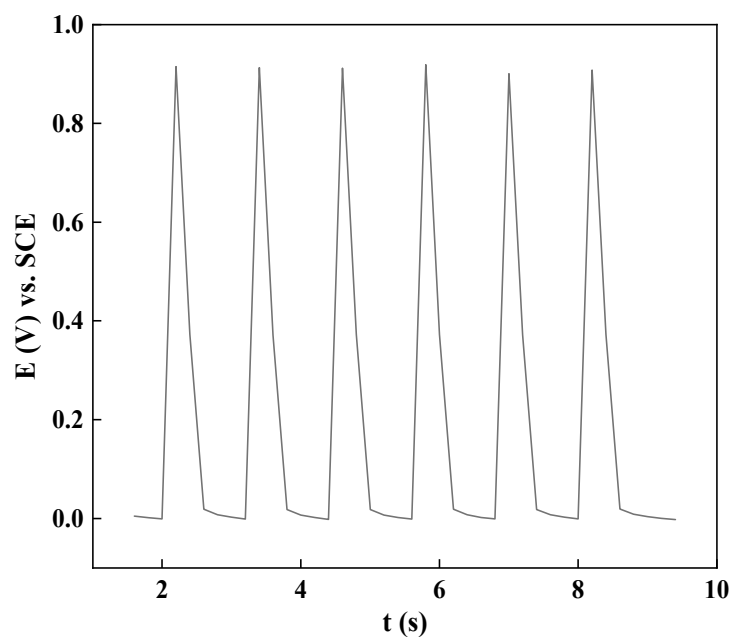


Figure 10. The charge-discharge curve of the prepared samples.

3.9. Oxidation of rGO Fabric in Air

To survey the electrochemical behavior and service life of rGO in a different environment, the samples are placed naturally in an air environment, and their resistivity is measured after 24, 48, and 72 h, respectively. The results are shown in Table 1. In this test, the prepared conductive fabrics are naturally oxidized in the air, and their conductivity is less affected within a certain time. Graphene oxide is a composite compound on the surface of graphene that adsorbs a variety of oxygen-containing functional groups. After chemical reduction (rGO), its conductivity gradually increases, and there is a certain band gap, which is manifested in semiconductor electrical properties. In reduced graphene oxide, the original complete graphene structure is isolated from the functional oxygen-containing defect region, resulting in the migration of electrons between the complete graphene phase and the defect region, which affects the conductivity of the materials. When GO is reduced to rGO, its structure has good stability in air and can be stored for a long time [50].

Table 1. The resistivity of rGO fabrics in air with different test times.

	The Original	24 h	48 h	72 h
Fabric resistivity $\rho/\Omega\cdot\text{m}$	6.44	6.57	6.88	6.91

3.10. Degradation of rGO Fabrics in 3% NaCl Solution

The rGO fabrics are immersed in 3 wt.% NaCl solution to study their degradation behavior, and the results are shown in Table 2. After immersion for 2 h, the resistivity almost remains unchanged. It indicates that although the test solution has certain erosion on the prepared conductive fabrics, it will no longer affect the fabric after 2 h of immersion. The weak binding of rGO and fabrics can be partially damaged, leading to a decline of resistivity, but rGO has good stability, so the conductive ability of rGO fabrics changes little with the increase of test time. So, rGO fabrics in 3 wt.% NaCl solution can only partly be corroded.

Table 2. The resistivity of conductive fabric soaked in NaCl solution for different times.

	Initial	1 h	2 h	3 h
Fabric resistivity $\rho/\Omega\cdot\text{m}$	6.39	15.23	21.32	21.64

SEM images of graphene conductive fabrics immersed in NaCl solution at different times are shown in Figure 11. It can be seen that small white particles can be found on the surface of the fabrics. The rGO film has a small layer spacing, and the Na^+ and Cl^- in the solution cannot enter the fabric [51], so the NaCl particles remain in the gaps of the conductive layer after drying, which also has some effect on the conductive properties of the fabrics.

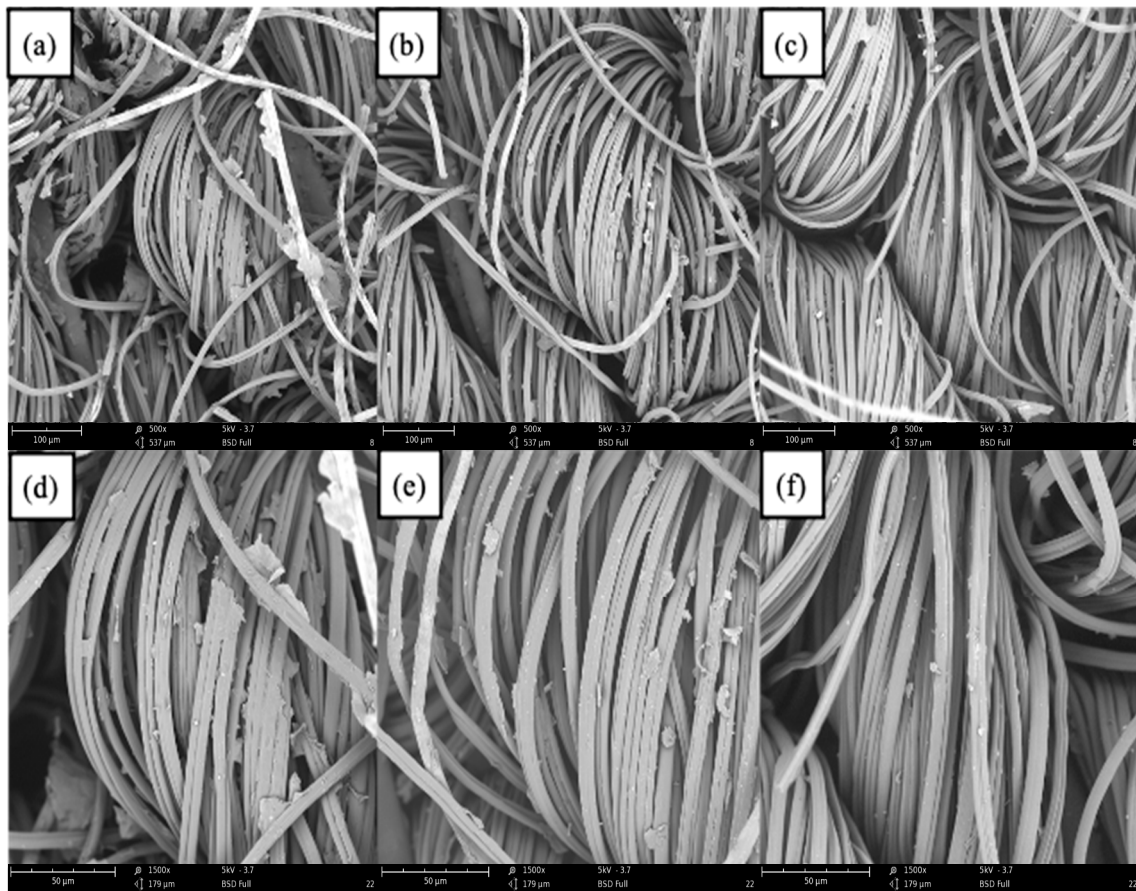


Figure 11. SEM images of graphene conductive fabric immersed in NaCl solution with a different time (a–c) are immersed for 1, 2, and 3 h, respectively, and imaged at 1500 \times magnification; images (d–f) are the part enlarge of images (a–c), respectively.

4. Conclusions

Graphene conductive fabrics and their technological parameter were investigated. The optimum number of dips for graphene conductive fabrics prepared by the dipping method was five. When the number of dips was less than five, the amounts of GO attached to the fabric were insufficient, so the resistivity was high. However, after dipping more than five times, the change in resistivity was not obvious. The best reduction temperature of GO conductive fabric prepared by the impregnation method was 95 °C. When the reduction temperature was below 95 °C, the reduction time of GO significantly increased. The optimum reduction time of conductive graphene fabrics was 40 min, and the optimum concentration of the reducing agent was 0.06 mol/L. CV and charge-discharge tests also showed the good electrical properties of the prepared samples. The prepared graphene conductive fabrics partly deteriorated in 3 wt.% NaCl solution because of the partial loss of their conductivity due to corrosion.

Author Contributions: Investigation, Conceptualization, Writing—original draft, W.X.; Data curation, Methodology, Y.J.; Investigation, G.H.; Visualization, Y.H.; Methodology, Y.Y.; Conceptualization, Y.N.; Data curation, J.Y.; Writing—review and editing, Project administration, Funding, Supervision, H.L. All authors have read and agreed to the published version of the manuscript.

Funding: This research was supported by the Guangdong Basic and Applied Basic Research Foundation (2019A1515011135), National Natural Science Foundation of China (51901253), and Fundamental Research Funds for the Central Universities (19lgzd18).

Institutional Review Board Statement: Not applicable.

Informed Consent Statement: Not applicable.

Data Availability Statement: Not applicable.

Conflicts of Interest: The authors declare no conflict of interest.

References

1. Habibi, P.; Moradi, G.; Moradi, A.; Golbabaie, F. A review on advanced functional photonic fabric for enhanced thermoregulating performance. *Environ. Nanotechnol. Monit. Manag.* **2021**, *16*, 100504. [[CrossRef](#)]
2. Sinha, A.; Dhanjai; Stavrakis, A.K.; Stojanović, G.M. Textile-based electrochemical sensors and their applications. *Talanta* **2022**, *244*, 123425. [[CrossRef](#)] [[PubMed](#)]
3. Zhang, Y.; Wang, H.; Lu, H.; Li, S.; Zhang, Y. Electronic fibers and textiles: Recent progress and perspective. *iScience* **2021**, *24*, 102716. [[CrossRef](#)] [[PubMed](#)]
4. Faruk, O.; Ahmed, A.; Jalil, M.A.; Islam, M.T.; Shamim, A.M.; Adak, B.; Hossain, M.; Mukhopadhyay, S. Functional textiles and composite based wearable thermal devices for Joule heating: Progress and perspectives. *Appl. Mater. Today* **2021**, *23*, 101025. [[CrossRef](#)]
5. Miah, M.R.; Yang, M.; Hossain, M.; Khandaker, S.; Awual, R. Textile-based flexible and printable sensors for next generation uses and their contemporary challenges: A critical review. *Sens. Actuators A Phys.* **2022**, *344*, 113696. [[CrossRef](#)]
6. Wen, J.; Xu, B.; Gao, Y.; Li, M.; Fu, H. Wearable technologies enable high-performance textile supercapacitors with flexible, breathable and wearable characteristics for future energy storage. *Energy Storage Mater.* **2021**, *37*, 94–122. [[CrossRef](#)]
7. Attia, N.F.; Elashery, S.E.; Zakria, A.M.; Eltaweil, A.S.; Oh, H. Recent advances in graphene sheets as new generation of flame retardant materials. *Mater. Sci. Eng. B* **2021**, *274*, 115460. [[CrossRef](#)]
8. Sattar, T. Current Review on Synthesis, Composites and Multifunctional Properties of Graphene. *Top. Curr. Chem.* **2019**, *377*, 10. [[CrossRef](#)]
9. Winter, M.; Brodd, R.J. What Are Batteries, Fuel Cells, and Supercapacitors? *Chem. Rev.* **2004**, *104*, 4245–4270. [[CrossRef](#)]
10. Hu, Q.; Nag, A.; Zhang, L.; Wang, K. Reduced graphene oxide-based composites for wearable strain-sensing applications. *Sens. Actuators A Phys.* **2022**, *345*, 113767. [[CrossRef](#)]
11. Htwe, Y.Z.N.; Mariatti, M. Printed graphene and hybrid conductive inks for flexible, stretchable, and wearable electronics: Progress, opportunities, and challenges. *J. Sci. Adv. Mater. Devices* **2022**, *7*, 100435. [[CrossRef](#)]
12. Ghosal, K.; Mondal, P.; Bera, S.; Ghosh, S. Graphene family nanomaterials- opportunities and challenges in tissue engineering applications. *FlatChem* **2021**, *30*, 100315. [[CrossRef](#)]
13. Yu, G.; Hu, L.; Vosgueritchian, M.; Wang, H.; Xie, X.; McDonough, J.R.; Cui, X.; Cui, Y.; Bao, Z. Solution-Processed Graphene/MnO₂ Nanostructured Textiles for High-Performance Electrochemical Capacitors. *Nano Lett.* **2011**, *11*, 2905–2911. [[CrossRef](#)]
14. Liu, W.-W.; Yan, X.B.; Lang, J.-W.; Peng, C.; Xue, Q.-J. Flexible and conductive nanocomposite electrode based on graphene sheets and cotton cloth for supercapacitor. *J. Mater. Chem.* **2012**, *22*, 17245. [[CrossRef](#)]
15. Krsihna, B.V.; Ravi, S.; Prakash, M.D. Recent developments in graphene based field effect transistors. *Mater. Today Proc.* **2020**, *45*, 1524–1528. [[CrossRef](#)] [[PubMed](#)]
16. Chakraborty, M.; Saleem, J.; Hashmi, M.; Ramadan, M. Graphene as a Material—An Overview of its Properties and Characteristics and Development Potential for Practical Applications. In *Encyclopedia of Smart Materials*; Olabi, A.-G., Ed.; Elsevier: Oxford, UK, 2022; pp. 81–95.
17. Pavia, M.; Alajami, K.; Estellé, P.; Desforges, A.; Vigolo, B. A critical review on thermal conductivity enhancement of graphene-based nanofluids. *Adv. Colloid Interface Sci.* **2021**, *294*, 102452. [[CrossRef](#)] [[PubMed](#)]
18. Wang, Y.; Peng, Y.; Wang, D.; Zhang, C. Wet deposition fluxes of total mercury and methylmercury in core urban areas, Chongqing, China. *Atmos. Environ.* **2014**, *92*, 87–96. [[CrossRef](#)]
19. Zhao, J.; Gao, T.; Li, Y.; He, Y.; Shi, Y. Two-dimensional (2D) graphene nanosheets as advanced lubricant additives: A critical review and prospect. *Mater. Today Commun.* **2021**, *29*, 102755. [[CrossRef](#)]
20. Vasseghian, Y.; Dragoi, E.-N.; Almomani, F.; Le, V.T. Graphene derivatives in bioplastic: A comprehensive review of properties and future perspectives. *Chemosphere* **2021**, *286*, 131892. [[CrossRef](#)]
21. Sengupta, J.; Adhikari, A.; Hussain, C.M. Graphene-based analytical lab-on-chip devices for detection of viruses: A review. *Carbon Trends* **2021**, *4*, 100072. [[CrossRef](#)]
22. Tian, M.; Du, M.; Qu, L.; Zhang, K.; Li, H.; Zhu, S.; Liu, D. Conductive reduced graphene oxide/MnO₂ carbonized cotton fabrics with enhanced electro-chemical, -heating, and -mechanical properties. *J. Power Sources* **2016**, *326*, 428–437. [[CrossRef](#)]
23. Mengal, N.; Sahito, I.A.; Arbab, A.A.; Sun, K.C.; Qadir, M.B.; Memon, A.A.; Jeong, S.H. Fabrication of a flexible and conductive lyocell fabric decorated with graphene nanosheets as a stable electrode material. *Carbohydr. Polym.* **2016**, *152*, 19–25. [[CrossRef](#)] [[PubMed](#)]
24. Maphiri, V.M.; Bakhom, D.T.; Sarr, S.; Sylla, N.F.; Rutavi, G.; Manyala, N. Low temperature thermally reduced graphene oxide directly on Ni-Foam using atmospheric pressure-chemical vapour deposition for high performance supercapacitor application. *J. Energy Storage* **2022**, *52*, 104967. [[CrossRef](#)]

25. Zhou, A.; Bai, J.; Hong, W.; Bai, H. Electrochemically reduced graphene oxide: Preparation, composites, and applications. *Carbon* **2022**, *191*, 301–332. [[CrossRef](#)]
26. Cao, J.; Wang, C. Highly conductive and flexible silk fabric via electrostatic self assemble between reduced graphene oxide and polyaniline. *Org. Electron.* **2018**, *55*, 26–34. [[CrossRef](#)]
27. Ma, Y.; Han, J.; Wang, M.; Chen, X.; Jia, S. Electrophoretic deposition of graphene-based materials: A review of materials and their applications. *J. Mater.* **2018**, *4*, 108–120. [[CrossRef](#)]
28. Bing, C.; Jiahao, Y.; Xiaoying, L.; Qi, J.; Guoping, W.; Linghua, J. Effects of reduction method on reduced graphene oxide and its electrochemical energy storage performance. *Diam. Relat. Mater.* **2021**, *114*, 108305. [[CrossRef](#)]
29. Aksu, Z.; Şahin, C.H.; Alanyalıoğlu, M. Fabrication of Janus GO/rGO humidity actuator by one-step electrochemical reduction route. *Sens. Actuators B Chem.* **2021**, *354*, 131198. [[CrossRef](#)]
30. Ren, J.; Wang, C.; Zhang, X.; Carey, T.; Chen, K.; Yin, Y.; Torrisi, F. Environmentally-friendly conductive cotton fabric as flexible strain sensor based on hot press reduced graphene oxide. *Carbon* **2017**, *111*, 622–630. [[CrossRef](#)]
31. Fogaça, L.Z.; Vicentini, J.C.M.; de Freitas, C.F.; de Souza, M.; Baesso, M.L.; Caetano, W.; Batistela, V.R.; Scaliante, M.H.N.O. Reduced graphene oxide impregnated in TiO₂ for photodegradation of dyes monitored in UV-LED mini-reactor. *Mater. Chem. Phys.* **2021**, *272*, 125020. [[CrossRef](#)]
32. Cai, W.; Ma, W.; Chen, W.; Liu, P.; Liu, Y.; Liu, Z.; He, W.; Li, J. Microwave-assisted reduction and sintering to construct hybrid networks of reduced graphene oxide and MXene for electromagnetic interference shielding. *Compos. Part A Appl. Sci. Manuf.* **2022**, *157*, 106928. [[CrossRef](#)]
33. Babaahmadi, V.; Montazer, M. Synthesis and daylight photocatalytic properties of graphene/self-doped tin oxide/silver ternary nanocomposite on fabric surface. *J. Photochem. Photobiol. A Chem.* **2022**, *422*, 113561. [[CrossRef](#)]
34. Tiwary, P.; Chatterjee, S.; Singha, S.; Mahapatra, R.; Chakraborty, A.K. Room temperature ethanol sensing by chemically reduced graphene oxide film. *FlatChem* **2021**, *30*, 100317. [[CrossRef](#)]
35. Pareek, A.; Sravan, J.S.; Mohan, S.V. Exploring chemically reduced graphene oxide electrode for power generation in microbial fuel cell. *Mater. Sci. Energy Technol.* **2019**, *2*, 600–606. [[CrossRef](#)]
36. Kurian, M. Recent progress in the chemical reduction of graphene oxide by green reductants—A Mini review. *Carbon Trends* **2021**, *5*, 100120. [[CrossRef](#)]
37. Mendes, I.S.; Prates, A.; Evtuguin, D.V. Production of rayon fibres from cellulosic pulps: State of the art and current developments. *Carbohydr. Polym.* **2021**, *273*, 118466. [[CrossRef](#)]
38. Zhu, X.; Li, Q.; Wang, L.; Wang, W.; Liu, S.; Wang, C.; Xu, Z.; Liu, L.; Qian, X. Current advances of Polyurethane/Graphene composites and its prospects in synthetic leather: A review. *Eur. Polym. J.* **2021**, *161*, 110837. [[CrossRef](#)]
39. Fugetsu, B.; Sano, E.; Yu, H.; Mori, K.; Tanaka, T. Graphene oxide as dyestuffs for the creation of electrically conductive fabrics. *Carbon* **2010**, *48*, 3340–3345. [[CrossRef](#)]
40. Lakra, R.; Kumar, R.; Sahoo, P.K.; Thatoi, D.; Soam, A. A mini-review: Graphene based composites for supercapacitor application. *Inorg. Chem. Commun.* **2021**, *133*, 108929. [[CrossRef](#)]
41. Zhao, C.; Shu, K.; Wang, C.; Gambhir, S.; Wallace, G.G. Reduced graphene oxide and polypyrrole/reduced graphene oxide composite coated stretchable fabric electrodes for supercapacitor application. *Electrochim. Acta* **2015**, *172*, 12–19. [[CrossRef](#)]
42. Pei, S.; Cheng, H.-M. The reduction of graphene oxide. *Carbon* **2012**, *50*, 3210–3228. [[CrossRef](#)]
43. Yue, B.; Wang, C.; Ding, X.; Wallace, G.G. Polypyrrole coated nylon lycra fabric as stretchable electrode for supercapacitor applications. *Electrochim. Acta* **2012**, *68*, 18–24. [[CrossRef](#)]
44. Kim, J.B.; Koo, S.H.; Kim, I.H.; Kim, J.G.; Jayaraman, B.; Lim, J.; Kim, S.O. Characteristic dual-domain composite structure of reduced graphene oxide and its application to higher specific capacitance. *Chem. Eng. J.* **2022**, *446*. [[CrossRef](#)]
45. Peng, W.; Sun, K.; Onck, P. Structure–property relations of three-dimensional nanoporous template-based graphene foams. *Extrem. Mech. Lett.* **2022**, *54*, 101737. [[CrossRef](#)]
46. Pasta, M.; La Mantia, F.; Hu, L.; Deshazer, H.D.; Cui, Y. Aqueous supercapacitors on conductive cotton. *Nano Res.* **2010**, *3*, 452–458. [[CrossRef](#)]
47. Yeasmin, S.; Talukdar, S.; Mahanta, D. Paper based pencil drawn multilayer graphene-polyaniline nanofiber electrodes for all-solid-state symmetric supercapacitors with enhanced cyclic stabilities. *Electrochim. Acta* **2021**, *389*, 138660. [[CrossRef](#)]
48. Er, X.; Chen, P.; Guo, J.; Hou, Y.; Yu, X.; Liu, P.; Bai, Y.; Zhan, Q. Enhanced energy-storage performance in a flexible film capacitor with coexistence of ferroelectric and polymorphic antiferroelectric domains. *J. Mater.* **2021**, *8*, 375–381. [[CrossRef](#)]
49. Rodriguez-Lopez, O.; Ruiz, E.G.; Polednik, A.J.; Duran-Martinez, A.C.; Garcia-Sandoval, A.; Voit, W.; Gutierrez-Heredia, G. Electrical characterization of flexible hafnium oxide capacitors on deformable softening polymer substrate. *Microelectron. Eng.* **2021**, *249*, 111618. [[CrossRef](#)]
50. Fan, L.; Wu, H.; Cao, M.; Zhou, X.; Peng, M.; Xie, W.; Liu, S. Enzymatic synthesis of collagen peptide–carboxymethylated chitosan copolymer and its characterization. *React. Funct. Polym.* **2014**, *76*, 26–31. [[CrossRef](#)]
51. Gao, Y.-F.; Wang, Y.; Zhou, D.; Lv, W.; Kang, F.-Y. Permselective graphene-based membranes and their applications in seawater desalination. *New Carbon Mater.* **2022**, *37*, 625–640. [[CrossRef](#)]